Influence of turbulent advection on a phytoplankton ecosystem with nonuniform carrying capacity

William J. McKiver and Zoltán Neufeld
School of Mathematical Sciences and Complex and Adaptive Systems Laboratory, University College Dublin, Belfield, Dublin 4, Ireland
(Received 16 March 2009; revised manuscript received 1 May 2009; published 2 June 2009)

In this work we study a plankton ecosystem model in a turbulent flow. The plankton model we consider contains logistic growth with a spatially varying background carrying capacity and the flow dynamics are generated using the two-dimensional (2D) Navier-Stokes equations. We characterize the system in terms of a dimensionless parameter, $\gamma \equiv T_B/T_F$, which is the ratio of the ecosystem biological time scales T_B and the flow time scales T_F. We integrate this system numerically for different values of γ until the mean plankton reaches a statistically stationary state and examine how the steady-state mean and variance of plankton depends on γ. Overall we find that advection in the presence of a nonuniform background carrying capacity can lead to very different plankton distributions depending on the time scale ratio γ. For small γ the plankton distribution is very similar to the background carrying capacity field and has a mean concentration close to the mean carrying capacity. As γ increases the plankton concentration is more influenced by the advection processes. In the largest γ cases there is a homogenization of the plankton concentration and the mean plankton concentration approaches the harmonic mean, $\langle 1/K \rangle^{-1}$. We derive asymptotic approximations for the cases of small and large γ. We also look at the dependence of the power spectra exponent, β, on γ where the power spectrum of plankton is $\propto k^{-\beta}$. We find that the power spectra exponent closely obeys $\beta = 1 + 2/\gamma$ as predicted by earlier studies using simple models of chaotic advection.

DOI: 10.1103/PhysRevE.79.061902 PACS number(s): 87.23.Cc, 47.27.T−, 47.63.mc

I. INTRODUCTION

Plankton is abundant throughout the oceans, seas, and lakes of the earth. As it is at the base of the food chain its distribution plays a major role in marine ecology at all levels. Its distribution, or spatial variability, is affected by a variety of factors, the availability of light and nutrients, the complex interactions between different types of plankton such as phytoplankton and zooplankton, and the ocean circulation which advects, stirs, and mixes the plankton ecosystem.

There have been many studies of a range of ecosystem models in an effort to explain the spatial heterogeneity (patchiness) of plankton distributions which have been observed in the ocean (see [1,2] for a review). The earliest models focused on the biological factors, i.e., the interdependence of phytoplankton, zooplankton, and nutrients with the ocean circulation being represented by diffusive processes [3–6]. More recently studies have taken into account the presence of advection. Beginning with Abraham [7], which considered an ecosystem model with time-dependent carrying capacity, phytoplankton, zooplankton with a maturation time, coupled to a two-dimensional turbulent flow. The resulting spectra showed that phytoplankton had a steeper spectral slope than zooplankton as a result of the fact that zooplankton has a longer reaction time than phytoplankton and thus there is more time for it to be mixed down to smaller scales. Birch *et al.* [8] approached the problem by focusing on a single-component model, i.e., phytoplankton, containing just logistic growth, advection and diffusion. In their model the growth rate is variable and they examined the survival-extinction transition when the growth rate is negative. When the system is in a survival regime they found upper and lower bounds on the biomass and productivity. Bracco *et al.* [9] examined how certain physical processes influence the relative spectral slopes of tracers at the sea surface. They find that for tracers with reaction/biological time scales longer than the flow time scale the dominant process in determining the spectral slope of the tracers is turbulent diffusion. When the supply is uncorrelated with the flow the behavior of the tracers is determined by the reaction time scale.

Despite the numerous studies of plankton patchiness it is still not clear what role the ocean transport processes play in the overall distribution of plankton. The importance of the biological and fluid dynamical parts usually vary for each model depending on the typical time scales associated with the ecosystem biological processes, T_B, and the fluid dynamical processes, T_F. The relative impact of these processes can be characterized by the nondimensional ratio $\gamma = T_B/T_F$. While the previous work mainly focused on plankton patchiness and has identified the effects of transport processes on the scaling properties of the fluctuations of the plankton distribution (e.g., spectral slope or roughness exponent), there has been relatively little work in understanding and quantifying the influence of mixing on the total or average concentration, which is however an important quantitative characteristic of marine ecosystems. We study the effect of the time scale ratio, γ, on the global statistical properties of the plankton distribution. We quantify the distribution of plankton using statistical measures such as the spatial mean or average concentration of plankton, defined as

$$\langle P(\mathbf{x},t) \rangle \equiv \frac{1}{A} \int \int P(\mathbf{x},t) dx dy, \tag{1}$$

where $P(\mathbf{x},t)$ is the plankton concentration and A is the area of the domain, and the variance

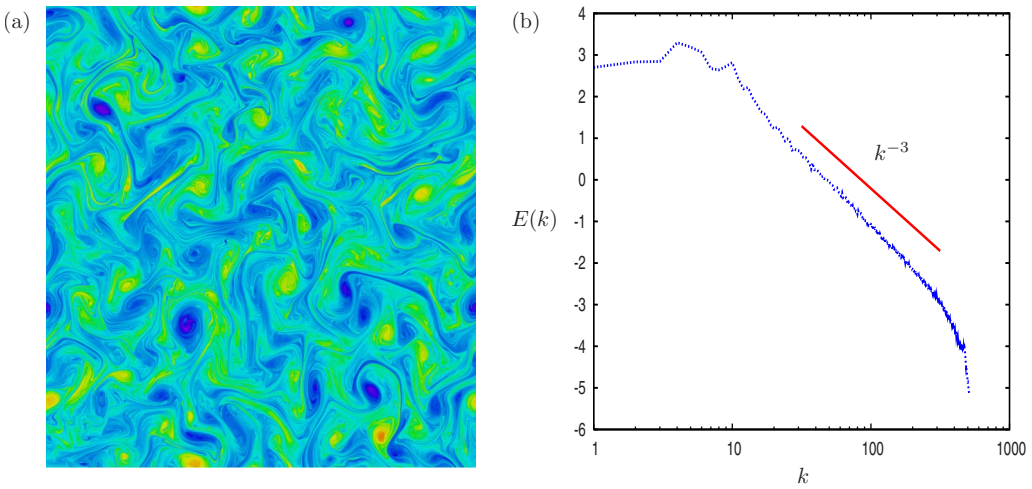

FIG. 1. (Color online) (a) The vorticity field at the statistical steady state in the doubly-periodic domain $x=[-\pi,\pi]$, $y=[-\pi,\pi]$. The minimum and maximum vorticity contours plotted are −0.7 (light/red) and 0.7 (dark/blue), respectively. (b) The energy spectra $E(k)$.

$$\mathrm{var}[P(\mathbf{x},t)] \equiv \langle (P(\mathbf{x},t) - \langle P(\mathbf{x},t)\rangle)^2\rangle, \tag{2}$$

which is a measure of the degree of fluctuation of concentration away from the mean. We will examine how these statistical quantities depend on the time scale ratio parameter γ.

We consider a minimal phytoplankton model, with logistic growth, advection, and a nonuniform carrying capacity, which is the simplest model in which mixing has nontrivial effects. The carrying capacity used varies in space. This reflects the spatial heterogeneity or patchiness of plankton seen in the ocean, where plankton blooms are found where nutrients are in abundance. Although this is a basic model, it provides a good test case for examining the competition between the biological and fluid dynamical processes and provides insights into more realistic cases. In the following section we introduce the model, both the fluid dynamical and plankton ecosystem components. In Sec. III we present the results from our simulations and analyze the limits of small and large γ, and we conclude in Sec. IV.

II. MODEL

A. Turbulence model

For our fluid dynamical model we use the two-dimensional (2D) incompressible Navier-Stokes equations,

$$\frac{\partial \zeta}{\partial t} + \boldsymbol{u}\cdot\boldsymbol{\nabla}\zeta = F + D, \tag{3}$$

where $\boldsymbol{u}(\mathbf{x},t)=(u,v)$ is the two-dimensional velocity field, $\zeta \equiv \partial v/\partial x - \partial u/\partial y$ is the vorticity field which is a scalar in 2D flows, D is the dissipation, and F is the forcing. The 2D Navier-Stokes equations are relevant to large-scale geophysical turbulence since the earth's rotation tends to inhibit vertical motions, making the dynamics quasi-two-dimensional [10,11]. The use of the 2D Navier-Stokes equations has an advantage over models using some effective diffusion or with an analytically prescribed velocity field since there are vortices present in the Navier-Stokes model. Many observations of the oceans reveal the presence of vortices which are often long lived and have an important effect on the horizontal transport and mixing processes (see [12] and references therein).

Equation (3) is solved on a doubly-periodic domain, $x=[-\pi,\pi]$ and $y=[-\pi,\pi]$, using a pseudospectral method with a fourth-order Runge-Kutta scheme for the time integration. The grid resolution used is $n_g^2=1024^2$. Here the dissipation is a combination of hyperdiffusion of the form $D_{hi}=-\nu\boldsymbol{\nabla}^8\zeta$, and linear friction given by $-\alpha\zeta$, which prevents accumulation of energy at the largest scales via the inverse cascade. The forcing is applied in spectral space at a wave number $k_f=10$ and is given by $F(k)=Ae^{i\phi}$, where A is the fixed forcing amplitude and ϕ is a random phase between 0 and 2π, which varies at each time step. We initialize our simulation with a smooth random vorticity field which we then integrate until a statistically stationary state is reached. This will be used as the initial condition for our simulations using the coupled plankton-fluid system. Figure 1(a) shows the vorticity field obtained in the statistical steady state.

The energy spectrum is shown in Fig. 1(b) and has a spectrum close to k^{-3} downscale of the forcing wave number as is predicted in the theory of 2D turbulence [13,14].

B. Ecosystem model

For the plankton dynamics we consider the simplest model that with advection produces a nontrivial spatial structure that is the logistic growth with nonuniform carrying capacity that is assumed to be smooth in space varying on large scales, which are comparable to the forcing scale

$$\frac{\partial P}{\partial t} + \boldsymbol{u}\cdot\boldsymbol{\nabla}P = rP\left(1 - \frac{P}{K(\mathbf{x})}\right), \tag{4}$$

where $P \equiv P(\mathbf{x},t)$ is the phytoplankton distribution, r is the maximum phytoplankton growth rate, $K(\mathbf{x}) \equiv K_0 - \delta\cos(x+y)$ is the nonuniform carrying capacity with minimum and maximum values of $K_0-\delta$ and $K_0+\delta$, respectively, and a mean value $\langle K(x,y)\rangle = K_0$. For our simulations we have set $K_0=3/2$ and $\delta=1/2$. Similar forms for the carrying capacity

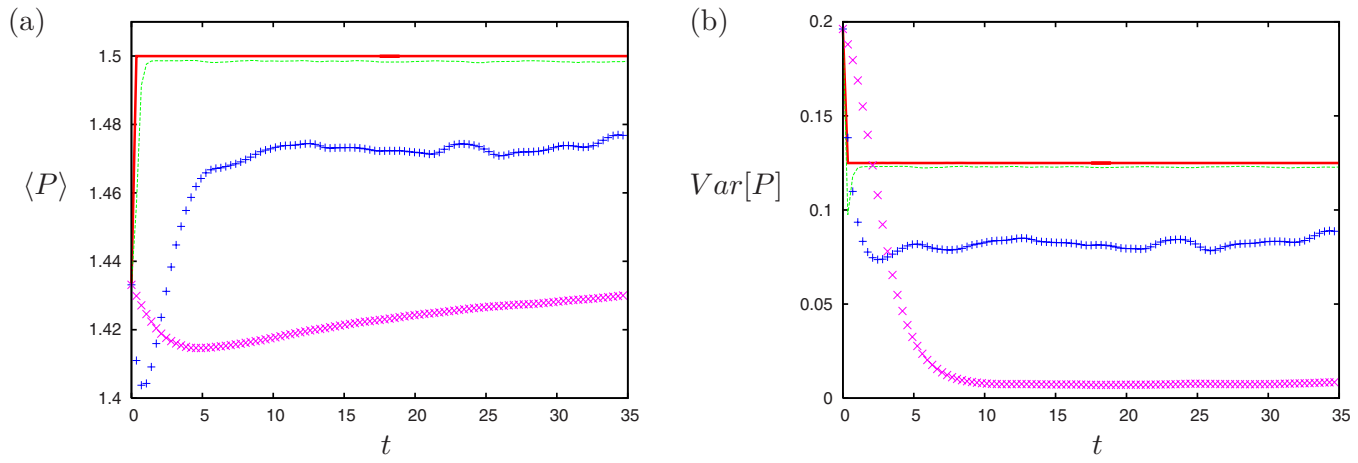

FIG. 2. (Color online) The evolution of (a) the mean plankton and (b) the variance of plankton. The different curves plotted are γ =0.018 (thick solid line), 0.18 (thin solid line), 1.8 (pluses), and 18 (crosses).

were used in Abraham [7] and Tzella and Haynes [15]. For the initial plankton distribution we choose a smooth random field with minimum and maximum values of 0.0 and $1.7K_0$, respectively. The ecosystem equations are integrated using a semi-Lagrangian scheme. The advecting fluid velocity is obtained from the pseudospectral method as described in the previous section, whereas the plankton dynamics is solved within fluid parcels, whose motion are tracked using the midpoint method and then calculated on grid points using bicubic interpolation (see [16,17] for details of the semi-Lagrangian method). We do not add diffusion explicitly in our model, but some numerical diffusion is always present as a result of using interpolation in the semi-Lagrangian scheme as is discussed in the work by Dritschel *et al.* [18].

For the plankton model the system can be characterized in terms of the parameter $\gamma \equiv T_B/T_F$, where the biological time scale is just the inverse of the growth rate, i.e., $T_B \equiv 1/r$, and we estimate the flow time scale from $T_F = L/U$, where L is the forcing length scale $L \equiv 2\pi/k_f$ and U is the root-mean-square velocity field. Thus γ is given by

$$\gamma = \frac{U}{rL}. \tag{5}$$

In our simulations we use just one fluid dynamical case which is provided by the initial conditions shown in Fig. 1. We fix the characteristic fluid time scale T_F to unity so that our time units are defined in units of T_F; however we examine a range of values of the time scale ratio γ by varying the growth rate.

III. RESULTS

A. Time evolution

We perform a number of simulations for a large range of values of the parameter γ. We integrate the equations until the mean plankton has reached a steady state, $\langle P \rangle = \langle P \rangle_S$, where $d\langle P \rangle_S/dt = 0$. Figure 2 shows the evolution of (a) the mean and (b) the variance of the plankton field for γ =0.018, 0.18, 1.8, and 18.

For each γ case there is an initial adjustment period before the mean plankton reaches a steady state. For γ=0.018 and 0.18 the mean plankton rapidly grows to the steady-state value. However for γ=1.8 and 18 the mean plankton initially decreases to a minimum before increasing again as it slowly approaches a steady state. The time taken for the mean plankton to reach a steady state appears to grow with γ. This makes reaching $\langle P \rangle_S$ as γ gets large very difficult numerically. The steady state of the variance of plankton however converges much more quickly.

In Fig. 3 we plot snapshots of the plankton field after $\langle P \rangle$ has reached the steady state, for a number of values of γ. For small γ [Figs. 3(a) and 3(b)] the plankton distribution is close to the background carrying capacity field $K(x,y)$, but as γ increases the plankton experiences turbulent advection. Effectively as the plankton moves it tries to relax to the local carrying capacity. When γ is small it is able to do this so quickly that while advection moves individual plankton parcels around, each parcel just takes on the value of the local carrying capacity field. For moderate values of γ the plankton parcels can only partially relax to the background carrying capacity before they are advected to another place. The spatial heterogeneity or patchiness seems to be a combination of the prescribed spatial structure of the carrying capacity and of the coherent structures within the flow. In the largest-γ cases the plankton field is almost uniformly distributed throughout the domain. The spatial structure of plankton seen in Fig. 3(d) looks typical of what is commonly seen in satellite images of plankton at the mesoscale, where advection processes and plankton biological processes occur on time scales of the same order of magnitude. However in the ocean the value of γ can widely vary depending on the region and the season.

Apart from the spatial structure the average of the plankton field also depends on γ. In Fig. 4 we plot the steady-state mean (a) and variance (b) of the plankton distribution as a function of γ.

The asymptotic values of $\langle P \rangle_S$ and var$[P]_S$ are marked by solid lines, which we will derive in the next section. Overall it appears that $\langle P \rangle_S$ and var$[P]_S$ decreases monotonically with γ.

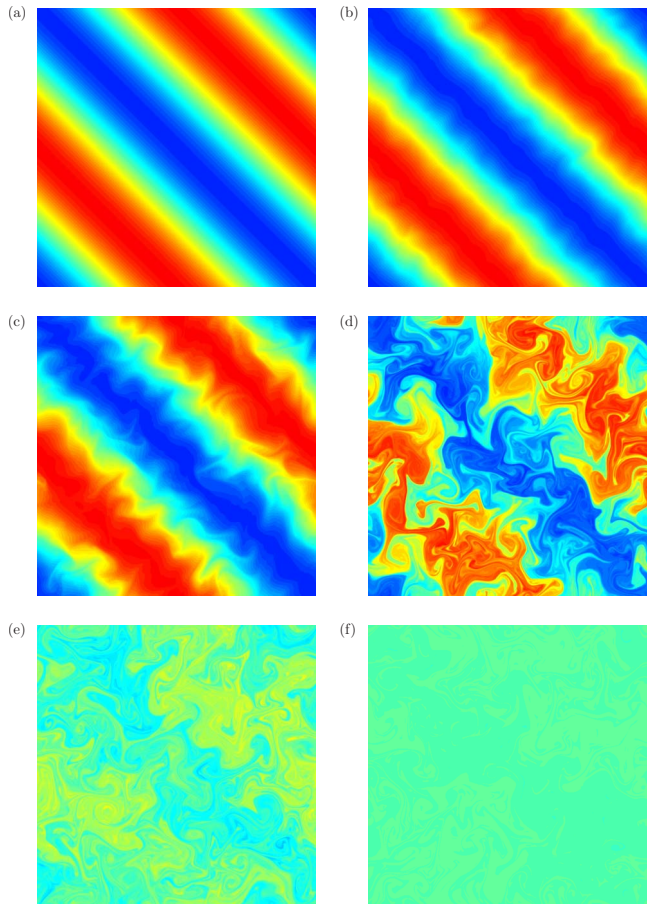

FIG. 3. (Color online) Contour plots of the equilibrium plankton fields for γ=0.0018, 0.06, 0.18, 1.8, 18, and 175 (going from left to right and from top to bottom). The minimum and the maximum contour values are 1.0 (dark/blue) and 2.0 (light/red).

To provide insight into this behavior it is worth examining the system in the limits as $\gamma \to \infty$ and $\gamma \to 0$ by expanding P in a perturbation expansion,

$$P = P_0 + \epsilon P_1 + \epsilon^2 P_2 + \cdots, \tag{6}$$

where ϵ is the small parameter (either γ or $1/\gamma$ depending on which limit is considered). It follows that the mean and variance of plankton are given by

$$\langle P \rangle = \langle P_0 \rangle + \epsilon \langle P_1 \rangle + \epsilon^2 \langle P_2 \rangle + \cdots, \tag{7}$$

$$\mathrm{var}[P] = \mathrm{var}[P_0] + 2\epsilon(\langle P_0 P_1 \rangle - \langle P_0 \rangle \langle P_1 \rangle) + \epsilon^2(\mathrm{var}[P_1] + 2(\langle P_0 P_2 \rangle - \langle P_0 \rangle \langle P_2 \rangle)) + \cdots. \tag{8}$$

Equation (4) can be rewritten in terms of the dimensionless parameter γ as

$$\frac{\partial P}{\partial t} + \boldsymbol{u} \cdot \nabla P = \frac{1}{\gamma} P \left(1 - \frac{P}{K}\right). \tag{9}$$

B. Small-γ limit

In the case $\gamma \to 0$, $\epsilon = \gamma$ and using Eq. (6) in Eq. (9) we obtain

$$\epsilon^0 : P_0 = K, \tag{10}$$

$$\epsilon^1 : P_1 = -\mathbf{u} \cdot \nabla K, \tag{11}$$

$$\epsilon^2 : P_2 = \frac{\partial \mathbf{u}}{\partial t} \cdot \nabla K + \mathbf{u} \cdot \nabla (\mathbf{u} \cdot \nabla K) - \frac{(\mathbf{u} \cdot \nabla K)^2}{K}. \tag{12}$$

Using the incompressibility of the flow ($\nabla \cdot \mathbf{u} = 0$) we can write $\mathbf{u} \cdot \nabla K = \nabla \cdot (\mathbf{u} K)$. Taking the spatial average of these equations, we can use that $\langle \nabla \cdot \mathbf{F} \rangle = 0$ for any vector function $\mathbf{F}$ in a periodic domain. Therefore the linear term vanishes after averaging. We can use the same property in the second-order term, and assuming that we are at a steady state where $d\langle P \rangle_S / dt = 0$, we obtain the perturbation expansion for $\langle P \rangle_S$, which is

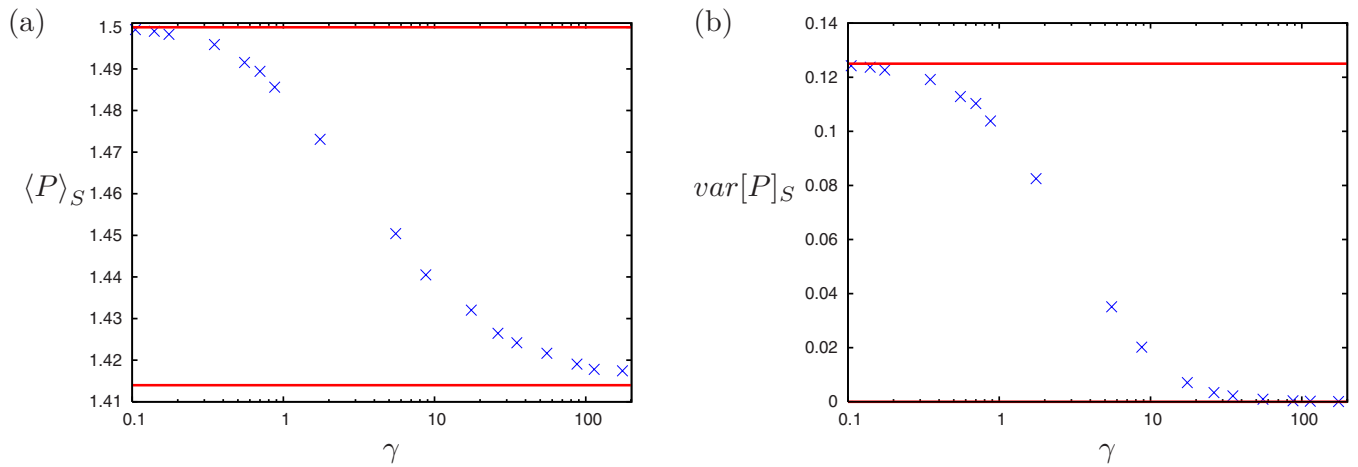

FIG. 4. (Color online) The equilibrium statistical values of (a) mean and (b) variance of plankton versus γ (in log scale). The solid lines in (a) and (b) represent the asymptotic values of $\langle P \rangle_S$ and $\mathrm{var}[P]_S$ in the two limits $\gamma \to 0$ and $\gamma \to \infty$.

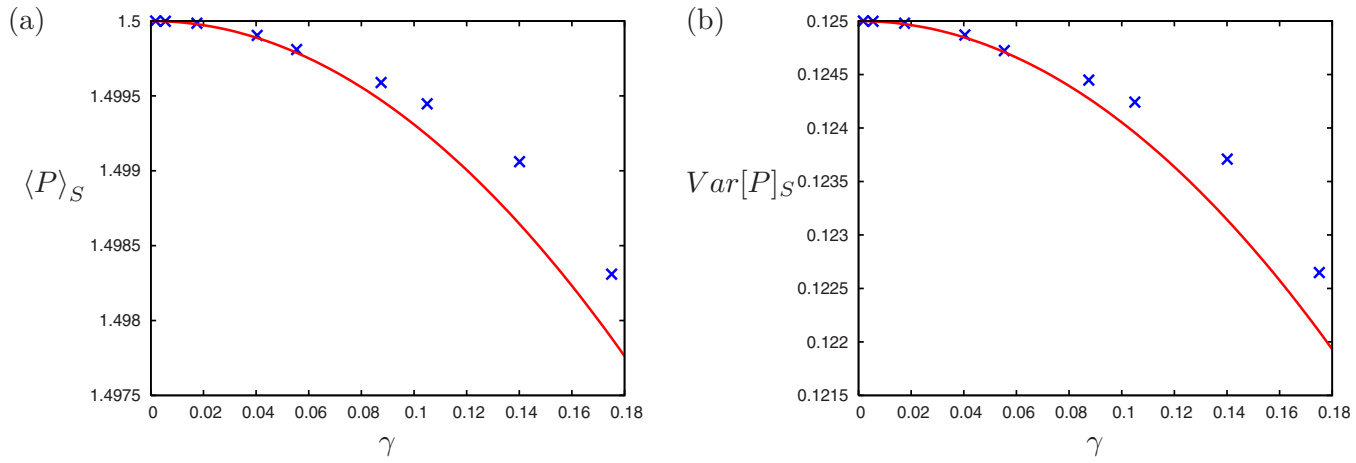

FIG. 5. (Color online) (a) and (b) show $\langle P\rangle_S$ and var$[P]_S$ as a function of γ for the small-γ limit. The crosses are the numerical results and the solid curves are the estimates given by the perturbation analysis.

$$\langle P\rangle_S = \langle K\rangle - \gamma^2\left\langle \frac{(\mathbf{u}\cdot\nabla K)^2}{K}\right\rangle + \cdots . \tag{13}$$

Since the turbulent velocity field is statistically homogeneous and isotropic and not correlated with the carrying capacity field we can apply the relation $\langle AB\rangle = \langle A\rangle\langle B\rangle$ to obtain

$$\langle P\rangle_S = \langle K\rangle - \frac{\gamma^2}{2}\left\langle \frac{|\nabla K|^2}{K}\right\rangle + \cdots , \tag{14}$$

where we have used the fact that $\langle u^2\rangle = 1$ since the dimensions are now contained in the parameter $\gamma = U/rL$. For the variance we obtain

$$\text{var}[P]_S = \text{var}[K] - \gamma^2\left[3\langle(\mathbf{u}\cdot\nabla K)^2\rangle - 2\langle K\rangle\left\langle\frac{(\mathbf{u}\cdot\nabla K)^2}{K}\right\rangle\right] + \cdots , \tag{15}$$

$$\approx \text{var}[K] - \gamma^2\left[\frac{3}{2}\langle|\nabla K|^2\rangle - \langle K\rangle\left\langle\frac{|\nabla K|^2}{K}\right\rangle\right] + \cdots . \tag{16}$$

Thus, in the case when the plankton growth rate is much faster than advection by the flow the average plankton concentration is equal to the average carrying capacity. For small positive γ the average and the variance decrease quadratically with a coefficient that is a measure of the magnitude of the advective flux across the isocontours of the carrying capacity distribution.

In Fig. 5 we compare the numerical results (crosses) against the estimates based on the perturbation analysis (solid curve) for small γ. For $\gamma \leq 0.06$ the perturbation analysis captures the full dynamics. However for greater values of γ the full solution diverges from the perturbation expansion, as one would expect as the perturbation approximation breaks down for large γ.

C. Large-γ limit

In the case $\gamma \to \infty$, $\epsilon = 1/\gamma$ and taking the perturbation expansion of P gives the equations

$$\epsilon^0 : \frac{\partial P_0}{\partial t} + \mathbf{u}\cdot\nabla P_0 = 0, \tag{17}$$

$$\epsilon^1 : \frac{\partial P_1}{\partial t} + \mathbf{u}\cdot\nabla P_1 = P_0\left(1 - \frac{P_0}{K}\right), \tag{18}$$

$$\epsilon^2 : \frac{\partial P_2}{\partial t} + \mathbf{u}\cdot\nabla P_2 = P_1\left(1 - 2\frac{P_0}{K}\right). \tag{19}$$

The first equation implies P_0 is materially conserved. However these equations are nontrivial and do not provide a way to determine the perturbation coefficients. Another approach to this case is to consider the equation for a Lagrangian particle $P(t)$, i.e.,

$$\frac{dP}{dt} = rP\left(1 - \frac{P}{K(t)}\right), \tag{20}$$

where now the carrying capacity varies with time along the Lagrangian trajectory. This equation can be written in integral form as

$$P(t) = \left[\int_0^t \frac{re^{r(\tau - t)}}{K(\tau)}d\tau + \frac{e^{-rt}}{P(0)}\right]^{-1}, \tag{21}$$

where $P(0)$ is the initial plankton concentration. If we consider the particle after a long time $t \gg 1/r$, we can neglect the term with the initial condition. Now we consider the limit when $r \ll 1$ and split the integral into intervals of time T, where $1 \ll T \ll 1/r$,

$$P(t) = \left[\sum_{n=0}^{n^*} re^{-rT(n-n^*)}\int_{nT}^{(n+1)T}\frac{1}{K(t)}dt\right]^{-1}, \tag{22}$$

where $n^* = t/T \gg 1$, and the integral

$$X \equiv \frac{1}{T}\int_{nT}^{(n+1)T}\frac{1}{K(t)}dt = \overline{\left[\frac{1}{K}\right]}_T \tag{23}$$

is just the Lagrangian mean of the function $1/K(t)$ (denoted by the overbar) over the time interval T, corresponding to the

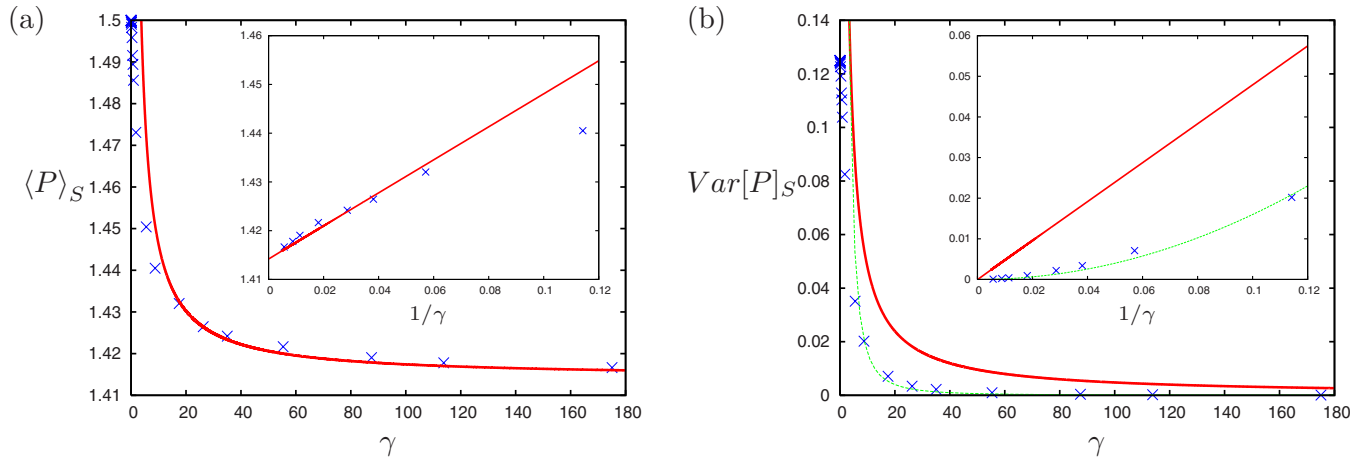

FIG. 6. (Color online) (a) and (b) show $\langle P\rangle_S$ and $\mathrm{var}[P]_S$ versus γ (main figure) and $1/\gamma$ (inset) for some large-γ values. The crosses are the numerical results and the thick solid curves are estimates given by the perturbation analysis. In (b) we also plot a fitted quadratic curve (thin line).

nth segment of the trajectory. The function $1/K(t)$ fluctuates within some bounded values about its mean which is given by its spatial average $\langle 1/K\rangle$. Due to the chaotic nature of the Lagrangian trajectories the fluctuations of $1/K(t)$ have a finite correlation time T_C that is a characteristic of the flow and may also depend on the length scale of the spatial structure of K. When T is much longer then this correlation time, X can be interpreted as the sum of independent identically distributed random variables, and by the Central Limit Theorem it has a Gaussian distribution with a mean $\langle 1/K\rangle$ and a variance of $\mathrm{var}[1/K]/n_c$, where $n_c=T/T_C$. Equation (22) can be rewritten as

$$P = \frac{1}{\sum_{k=0}^{\infty} rTe^{-rkT}X_k} = \frac{1}{Y}, \tag{24}$$

where $k=n^*-n$ and since $rT \ll 1$ the upper limit can be extended to infinity. Y is thus a linear combination of Gaussian random variables, which is thus also Gaussian. In the $r\to 0$ (i.e., large-γ) limit the plankton field is almost uniform and the dominant contribution comes from the region around the mean. We can Taylor expand this function about its mean $\langle Y\rangle \equiv Y_0$ to get

$$P = \frac{1}{Y_0} - \frac{(Y-Y_0)}{Y_0^2} + \frac{(Y-Y_0)^2}{Y_0^3} + \cdots. \tag{25}$$

Thus the mean and the variance of P are given by

$$\langle P\rangle = \frac{1}{Y_0} + \frac{\mathrm{var}[Y]}{Y_0^3} + \cdots, \tag{26}$$

$$\mathrm{var}[P] = \frac{\mathrm{var}[Y]}{Y_0^4} + \cdots, \tag{27}$$

where Y_0 is

$$Y_0 = \sum_{k=0}^{\infty} rTe^{-rTk}\langle X\rangle, \tag{28}$$

but this is a geometric series and can be estimated as

$$\sum_{k=0}^{\infty} rTe^{-rTk} = \frac{rT}{1-e^{-rT}} \approx \frac{rT}{1-1+rT} = 1, \tag{29}$$

so that $Y_0=\langle X\rangle=\langle 1/K\rangle$. The variance of Y is

$$\mathrm{var}[Y] = \mathrm{var}\left[\sum_{k=0}^{\infty} rTe^{-rTk}X\right], \tag{30}$$

$$= \sum_{k=0}^{\infty} r^2T^2e^{-2rTk}\mathrm{var}[X], \tag{31}$$

$$\approx \frac{1}{2}rT_C\mathrm{var}[1/K]. \tag{32}$$

So finally we have

$$\langle P\rangle = \left\langle \frac{1}{K}\right\rangle^{-1} + \left[\frac{\mathrm{var}[1/K]}{2\langle 1/K\rangle^3}\right]\frac{a_T}{\gamma} + \cdots, \tag{33}$$

$$\mathrm{var}[P] = \left[\frac{\mathrm{var}[1/K]}{2\langle 1/K\rangle^4}\right]\frac{a_T}{\gamma}, \tag{34}$$

where $a_T \equiv T_C/T_F$. So in the large-γ limit $\langle P\rangle_S$ decreases with γ and the asymptotic value is the harmonic mean of the carrying capacity $\langle 1/K\rangle^{-1}$, which by the Jensen's inequality is always smaller than the average carrying capacity for any nonuniform K. The variance goes to zero indicating that the plankton distribution is close to uniform when the flow is much faster than the plankton growth rate as in the numerical simulations.

In Fig. 6 we examine the large γ limit. In the inset we plot $\langle P\rangle_S$ and $\mathrm{var}[P]_S$ against $1/\gamma$ to show the dependence on $1/\gamma$ in the large-γ limit, as was found in the perturbation analysis.

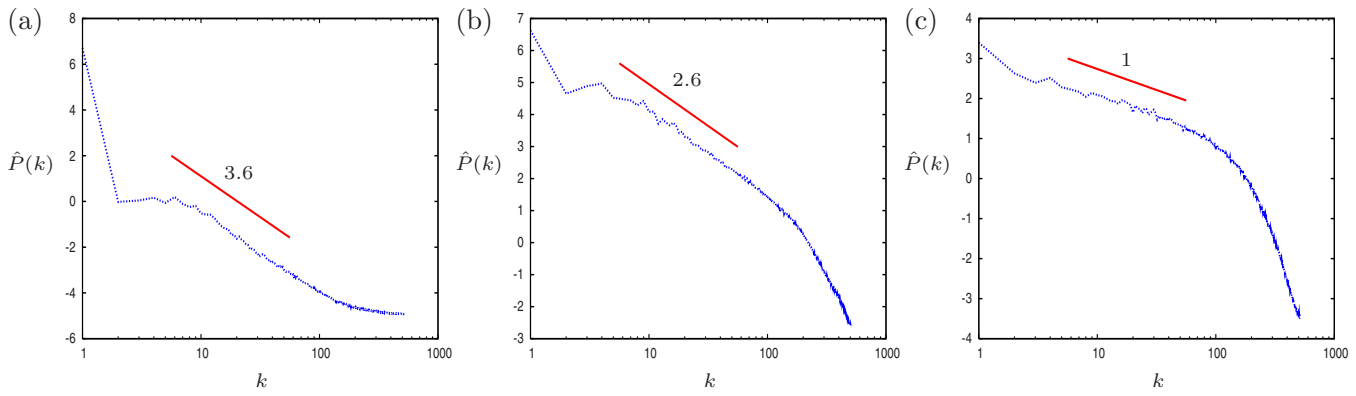

FIG. 7. (Color online) Equilibrium plankton spectra for γ=(a) 0.18, (b) 0.6, and (c) 114. Spectral slopes β are indicated where $P(k) \propto k^{-\beta}$.

In order to estimate the correlation time T_C we use a Lagrangian method, which determines how the value of the function $1/K$ varies along a Lagrangian trajectory. We find that $T_C \approx 8T_F$, which is consistent with our system where the vortex sizes are smaller than the bands over which the carrying capacitance varies. For the mean plankton the theory agrees with the numerical results; however there are significant differences for the estimate of the variance of plankton from the numerical results. In fact the dependence on $1/\gamma$ appears to be quadratic for the variance, as is shown in Fig. 6(b) where we have fitted a quadratic curve (green line). The reason for the disparity between the results and the theory for the variance is due to the fact that in this Lagrangian approximation we completely neglected the effect of numerical diffusion. Although this has a negligible effect on the average plankton concentration it leads to a numerical dissipation of the concentration fluctuations, which becomes important in the singular large-γ limit, when the plankton field behaves almost like a passive scalar. Since this is not included in the Lagrangian representation, our prediction overestimates the variance of the plankton concentration in the large-γ limit. This has been confirmed by direct Lagrangian numerical simulations for the plankton dynamics using Eq. (20), which give linear dependence on $1/\gamma$ and larger values of the variance than the solution of the full system when γ is very large.

D. Power spectrum

In order to see how the spatial distribution of the equilibrium plankton is affected by changes in γ, it is useful to look at the power spectra of the equilibrium plankton fields. In Fig. 7 we show the spectra for the cases γ=0.18, 0.6, and 114.

In each case the solid lines indicate the spectral slopes which are $\propto k^{-\beta}$. For the case γ=0.18, most of the plankton is concentrated at small wave numbers; this is consistent with the carrying capacity concentration field. For larger values of γ the larger wave numbers become more significant and the spectrum approaches a k^{-1} slope as is found for the spectrum of passive tracers in the so-called Batchelor regime.

In the work by Neufeld *et al.* [19] (also see [20]) the exponent β for a decaying chemical field was found to be $\beta = 1 + 2b/\lambda_F$, where b is the decay rate of the chemical and λ_F is the Lyapunov exponent of the flow. In our case the stability of the steady state is controlled by the growth rate r instead of the decay rate b. This theory applies when there is a single well defined Lyapunov exponent; however in our case measurements of the Lyapunov exponent over a finite time using an ensemble of initial conditions reveal a range of values for the Lyapunov exponent. This distribution of Lyapunov exponents may be due to the presence of long-lived coherent structures, which can restrict the dispersion of nearby trajectories which are within these vortices. Chertkov *et at* [21], Nam *et al.* [22], and Neufeld *et al.* [23] showed that such a distribution of the Lyapunov exponents can modify the formula for the exponent β. For our case we have found that the formula is better approximated when we use the inverse of the flow time scale instead of the Lyapunov exponent, i.e., $1/T_F = U/L$. Thus in terms of the parameter γ we obtain the expression

$$\beta = 1 + \frac{2}{\gamma}. \tag{35}$$

In Fig. 8 we compare this expression (solid curve) with the results obtained from the numerically simulations (crosses).

This simple formula seems to give a remarkably accurate prediction of the spectral slope β as a function of γ.

IV. CONCLUSIONS

In this paper we examined a basic coupled plankton-fluid dynamical system in order to understand the relative importance of advective transport and biological plankton growth. Overall we found that advection in the presence of a nonuniform background carrying capacity can lead to very different plankton distributions depending on the time scale ratio γ. For small γ the plankton concentration is very similar to the background carrying capacity field and has a mean concentration close to the mean carrying capacity field, i.e., $\langle K \rangle$. As γ increases the plankton concentration is more influenced by the advection processes and the structures within the flow, such as vortices. In the largest-γ cases there is a homogenization of the plankton concentration, only feeling the average effect of the carrying capacity field. In the large-γ limit the

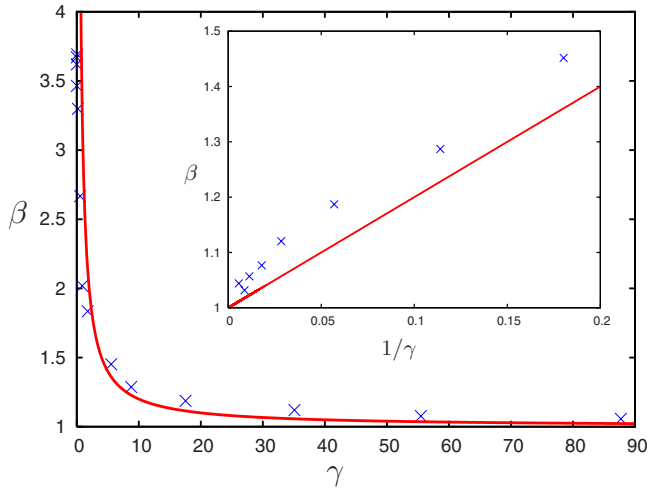

FIG. 8. (Color online) Plot of the spectral slope versus the γ (main figure) and $1/\gamma$ (inset). The crosses are the numerical results and the solid lines are the estimate based on $\beta=1+2/\gamma$.

mean plankton concentration approaches $\langle 1/K\rangle^{-1}$. Our analysis of the power spectra shows that as γ increases the plankton behaves more like a passive tracer where the spectrum is proportional to k^{-1}. Overall the mean plankton is bounded between the upper limit $\langle K\rangle$ and the lower limit $\langle 1/K\rangle^{-1}$. For our choice of the carrying capacity field the difference in these limits is small; however in general the gap between these limits can be much greater. For instance if the carrying capacity field is high over most of the domain, but has small regions of very low carrying capacity, this would give rise to a large value for the mean but a very small value for the harmonic mean $\langle 1/K\rangle^{-1}$ and in this case the total amount of plankton is very sensitive to the stirring rate or the scale ratio γ.

The ecosystem model used here is very simple. It would be interesting to apply a similar analysis to a more realistic ecosystem such as a phytoplankton-zooplankton or nutrient-phytoplankton-zooplankton (NPZ) model. In Pasquero [24] the dependence of the mean phytoplankton concentration on the time scale ratio was found numerically for a NPZ system. In that case the mean plankton concentration monotonically increased with γ, unlike in our case where it decreases with increasing γ. This also suggests the possibility that the mean plankton may not depend monotonically on γ for certain ecosystem models, so that there could be an intermediate value of γ for which the phytoplankton/zooplankton has a maximum. A recent study [25] analyzed the horizontal mixing properties of two ocean upwelling systems using finite-size Lyapunov exponent analysis. They found that horizontal stirring and mixing have a negative correlation with biological activity. This is what we qualitatively find in our simple model where the phytoplankton decreases with flow speed.

In our model we were able to approximate the solutions in the limits when γ is very small or very large. However the main patchiness observed in the spatial structure of plankton seems to occur for intermediate values of γ. It would be useful to find a means of studying these cases using some analytical or reduced model.

ACKNOWLEDGMENTS

Support for this research has come from the Irish Research Council for Science, Engineering and Technology and the Science Foundation of Ireland. Also we wish to acknowledge the SFI/HEA Irish Centre for High-End Computing (ICHEC) for the provision of computational facilities and support.

[1] A. P. Martin, Prog. Oceanogr. **57**, 125 (2003).
[2] M. Lévy, Lect. Notes Phys. **744**, 219 (2008).
[3] J. G. Skellam, Biometrika **38**, 196 (1951).
[4] H. Kierstead and L. B. Slobodkin, J. Mar. Res. **12**, 141 (1953).
[5] R. Bainbridge, Biophys. Rev. Lett. **32**, 91 (1957).
[6] K. L. Denman, A. Okubo, and T. Platt, Limnol. Oceanogr. **22**, 1033 (1977).
[7] E. R. Abraham, Nature (London) **391**, 577 (1998).
[8] D. A. Birch, Y. K. Tsang, and W. R. Young, Phys. Rev. E **75**, 066304 (2007).
[9] A. Bracco, S. Clayton, and C. Pasquero, J. Geophys. Res. **114**, C02001 (2009).
[10] J. Pedlosky, *Geophysical Fluid Dynamics* (Springer, New York, 1987).
[11] G. K. Vallis, *Atmospheric and Oceanic Fluid Dynamics: Fundamentals and Large-Scale Circulation* (Cambridge University Press, Cambridge, 2006).
[12] A. Provenzale, Annu. Rev. Fluid Mech. **31**, 55 (1999).
[13] R. H. Kraichnan, Phys. Fluids **10**, 1417 (1967).
[14] P. Tabeling, Phys. Rep. **362**, 1 (2002).
[15] A. Tzella and P. H. Haynes, Biogeosciences **4**, 173 (2007).
[16] P. Bartello and S. Thomas, Mon. Weather Rev. **124**, 2883 (1996).
[17] C. Temperton and A. Staniforth, Q. J. R. Meteorol. Soc. **113**, 1025 (1987).
[18] D. Dritschel, L. Polvani, and A. Mohebalhojeh, Mon. Weather Rev. **127**, 1551 (1999).
[19] Z. Neufeld, C. López, and P. H. Haynes, Phys. Rev. Lett. **82**, 2606 (1999).
[20] E. Hernández-García, C. López, and Z. Neufeld, Chaos **12**, 470 (2002).
[21] M. Chertkov, Phys. Fluids **10**, 3017 (1998).
[22] K. Nam, T. M. Antonsen, P. N. Guzdar, and E. Ott, Phys. Rev. Lett. **83**, 3426 (1999).
[23] Z. Neufeld, C. López, E. Hernández-García, and T. Tél, Phys. Rev. E **61**, 3857 (2000).
[24] C. Pasquero, Geophys. Res. Lett. **32**, L17603 (2005).
[25] V. Rossi, C. López, J. Sudre, E. Hernández-García, and V. Garçon, Geophys. Res. Lett. **35**, L11602 (2008).